

# Design and Analysis of Helical Flagella Propelled Nanorobots

Subramanian S.<sup>1</sup>, J. S. Rathore<sup>1</sup>, and N. N. Sharma<sup>1,\*</sup>

<sup>1</sup>Mechanical Engineering Department, Birla Institute of Technology and Science, Pilani, India

**Abstract** — Advancement in the field of nanorobotics has been facilitated by the current advances in nano-bio-technology and nanofabrication methods. The important uses of nanorobots are in advancing medical technology, healthcare and environment monitoring. In bio-medical applications, nanorobots need to swim in biological fluids flowing in narrow channels of few hundred nanometer size. The dominating effects in nanometer size domains are increased apparent viscosity and low Reynolds numbers which makes the design of a propulsion mechanism a challenging task. Micro and nano size biological organisms move by generating planar waves or rotating helical flagella. In the present work, design of propulsion with helical flagella is proposed and a generalized analytical model is developed, simulated and discussed. The performance parameters of the developed model viz. velocity and efficiency have been computed based on resistive force theory and compared with those of the model available in literature. Improved performance, feasibility and generality of the developed flagellar model have been discussed.

**Keywords** — Flagellar hydrodynamics, Helical flagellar propulsion, Nanorobotics, Resistive Force Theory

## I. INTRODUCTION

Miniaturization has many appealing advantages and has attracted a lot of attention with improvements in enabling technologies like VLSI, MEMS and Nanotechnology. Small size of the order of few nanometers to a few micrometers is itself advantageous, because of being comparable to some biological dimensions. Miniaturized robots can be used for various tasks where the main challenge has been the size. The most important of the possible uses of nanorobots is in the field of medicine where it has the potential to revolutionize the methods of diagnosis and treatments for diseases like cancer. The existing methods like radiation therapy are not specific and have effects on other non cancerous cells of the body. For similar applications, nanorobots have to move through body fluids flowing in narrow channels of the body. The motion of nanorobots in narrow channels is eclipsed by an increase in apparent viscosity, low Reynolds number and negligible inertia compared to viscous effects. The important qualities desirable for nanorobots are high velocity, efficiency, specificity, controllability and a simple propagation mechanism that can be realized with miniaturized parts. In the realization of nanorobots, other challenges are wearing and friction, significant Brownian motion due to thermal agitation and non rigidity in nano domains due to which it is more propitious to swim or fly compared to crawling and walking [1]. Inspired by the fact that microorganisms existing in nature function expeditiously under these circumstances, scientists and engineers have shown a great interest to conceptualize, model, analyze and make micro-sized swimmers that can move in body fluids [1-5]. Efficiency of propulsion is extremely low but

is not a cause of concern considering the abundance of energy available to the micro and nano sized biological organisms [2]. Considering an artificial nanorobot, energy available on board and efficiency of propulsion are critical for practical uses of these nano devices. Two major approaches to model propulsion in nano domains are Resistive Force Theory (RFT) and Slender Body Theory (SBT). The SBT is more accurate, but it is computationally intensive compared to RFT [3]. RFT has been used in published literature to model and analyze promising propulsion mechanisms achieved by planar or helical ciliary and flagellar motion. Gray and Hancock [4] developed a general theory for the propulsion of spermatozoa based on resistive forces generated due to planar bending waves. In [6], Honda *et al.* proposed a new method for propulsion by rotating a ferromagnetic helical coil using magnetic field. Despite the limitations such as low velocity, it circumvents the problem of incorporating an efficient motoring mechanism within the head. Biomimetic propulsion mechanism was considered by Behkam *et al.* [7], where the performance has been estimated by modeling the dynamics of motion. Inspired by the motility mechanism of prokaryotic and eukaryotic microorganisms with peritrichous flagellation, models for the propulsion of microrobots have been developed and validated using a scaled up model [8].

In the planar bending wave model, elements of the flagella undergo opposite strains often and energy has to be generated locally for sustaining the same amplitude throughout the length of the tail. The reversible straining is less in case of helical flagellar propulsion mechanism. Behkam *et al.* [7-8] presented a Biomimetic propulsion model by using RFT for analyzing the performance of a uniform amplitude helical flagellum. The flagellum is considered as a long thin (~20 nm thick), helix (2.5  $\mu\text{m}$  pitch, 0.5  $\mu\text{m}$  diameter) that rotates at a speed of ~100 Hz. The helix of the flagellum is considered to have a constant amplitude and constant pitch in [7-8]. The influence of varying amplitude and pitch needs to be explored for improved performance of the propulsion mechanism. In the present work, a generalized case of helical wave mechanism is modeled where the amplitude ( $y$ ) varies along the length of the flagella. The rotation of the helical flagella about the longitudinal axis, results in a net forward thrust, in viscous domains, which propels the robot forward. The mathematical model for the forces, velocity, and efficiency, considering a general case of the helical flagellar mechanism, is developed. The investigation on performance parameters for the linearly varying amplitude helical flagellar mechanism is done and is compared with the constant amplitude model. The results are discussed for improved efficiency of propulsion for the nanorobot. The results obtained show that there is a scope for significant improvement in performance by varying the amplitude and pitch. The present work is organized into three more sections.

\*Contact author e-mail: nns@bits-pilani.ac.in

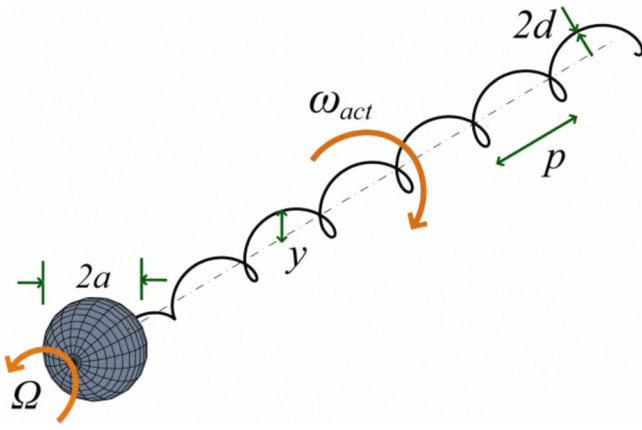


Fig. 1. Schematic of a nanorobot with varying amplitude helical flagellum

In the next section, methodology and modeling of the proposed mechanism is presented. In section III, simulation and significant results of the developed model are discussed. In the last section, conclusions and scope for future work are mentioned.

## II. METHODOLOGY AND MODELING

Surface area to volume ratio increases with reduction in size and surface effects become prominent in nano domains. Dimensions of the nanorobot depend on its application requirements and the capability of the available fabrication technology. Small dimensions of the robot and the nature of flow in small channels results in very low Reynolds numbers. Viscous effects dominate the inertial forces and the flow is termed as Stokes flow. Models for nanorobot propulsion have been developed considering the conditions of dominating viscous forces, low Reynolds number and negligible inertia.

The hydrodynamics of flagella are analyzed using RFT to model the propulsion of nanorobots. The components of drag force that are generated depend on the components of the velocity along the respective directions. The developed model of nanorobot propulsion is valid for low Reynolds numbers where inertial forces are negligible.

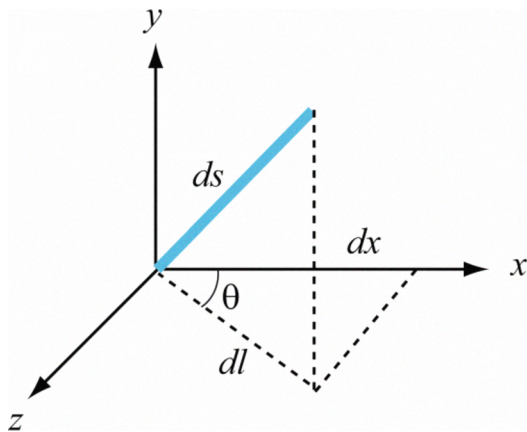


Fig. 2. A small element of the varying amplitude helix

Fig. 1 shows the schematic of the nanorobot with a variable amplitude helical flagellum and an inert head. The diameter of the head is denoted as  $2a$ , the thickness of the filament is  $2d$ , the uniform pitch of the helix is  $p$  and the amplitude,  $y$  varies along the longitudinal axis,  $x$ . A small element of the helix is shown in Fig. 2 where,  $y$  is the radial axis,  $x$  is the longitudinal axis and the length of the element is  $ds$ . The instantaneous pitch angle,  $\theta$ , is given by

$$\tan \theta = \frac{2\pi y}{p} \quad (1)$$

From Fig. 2 the length of the element is obtained as,

$$ds = \sqrt{1 + \cos^2 \theta \left( \frac{dy}{dx} \right)^2} \frac{dx}{\cos \theta} \quad (2)$$

The angle between  $ds$  and  $dl$  is very small when the gradient of the amplitude is small and the tangential component of the drag force,  $\delta L$ , acting on the element is approximated as

$$\delta L = C_L (V_\theta \sin \theta + V_x \cos \theta) \delta s \quad (3)$$

and the normal component of the drag force,  $\delta N$ , is equal to

$$\delta N = C_N (V_\theta \cos \theta - V_x \sin \theta) \delta s \quad (4)$$

where  $V_x$  is the forward velocity and  $V_\theta$  is the equivalent translational velocity of the element resulting from the rotation about the longitudinal axis.  $C_L$  and  $C_N$  are the coefficients of resistance or the drag coefficients along the tangential and normal directions which relate the velocity and the drag force along the respective directions. The expressions for  $C_L$  and  $C_N$  for a single flagellum with free ends are given by [3]

$$C_L = \frac{2\pi\mu}{\ln\left(\frac{2p}{d}\right) - \frac{1}{2}} \quad (5)$$

$$C_N = \frac{4\pi\mu}{\ln\left(\frac{2p}{d}\right) + \frac{1}{2}} \quad (6)$$

From equations (1) through (4), the forward thrust due to the small element is obtained as

$$\delta F_x = \left[ \frac{(C_N - C_L)V_\theta \tan \theta - V_x(C_L + C_N \tan^2 \theta)}{1 + \tan^2 \theta} \right] \delta s \quad (7)$$

Under steady state conditions, the magnitude of the thrust force generated by the entire helical tail is equal to the drag experienced by the head:

$$F_{thrust} = \int dF_x = F_{head} \quad (8)$$

The motor mechanism inside the head rotates the shaft with an angular velocity  $\omega$ . For the resultant torque applied on the robot to be zero, the head rotates in the opposite direction with an angular velocity  $\Omega$  [8]. Therefore, the helical filament rotates with an absolute angular velocity of  $\omega_{act} = \omega - \Omega$ .

Considering only small gradients in amplitude, the torque required to rotate the small element shown in Fig. 2 is given as

$$\delta M_\theta = \left[ \frac{V_x(C_N - C_L)\tan\theta + V_\theta(C_L + C_N \tan^2\theta)}{1 + \tan^2\theta} \right] y \delta x \quad (9)$$

The drag experienced by a spherical head of radius  $a$ , in a medium with viscosity  $\mu$  is given as

$$F_{head} = 6\pi\mu a V_x \quad (10)$$

and the torque required to rotate the head is given by

$$M_{head} = 8\pi\mu a^3 \Omega \quad (11)$$

The steady velocity of the nanorobot,  $V_x$ , is calculated from equations (5) through (8) and (10). Efficiency of the system is computed as the ratio of the useful power developed (for axial motion) to the total input power required for spinning the head and the flagella:

$$\eta = \frac{F_{thrust} V_x}{M_\theta \omega_{act} + M_{head} \Omega} \quad (12)$$

### III. SIMULATION AND RESULTS

The simulations of the developed efficiency and forward velocity models are done in MATLAB considering dimensions and angular velocity of the helix as user inputs. A flagellum with 20 turns is considered for simulations. The viscosity of blood through which the nanorobot is assumed to propagate is considered as 4 mPa.s. A Number of helical profiles are considered for flagellar design; the two profiles with constant and linearly varying amplitude are presented and discussed in the present work.

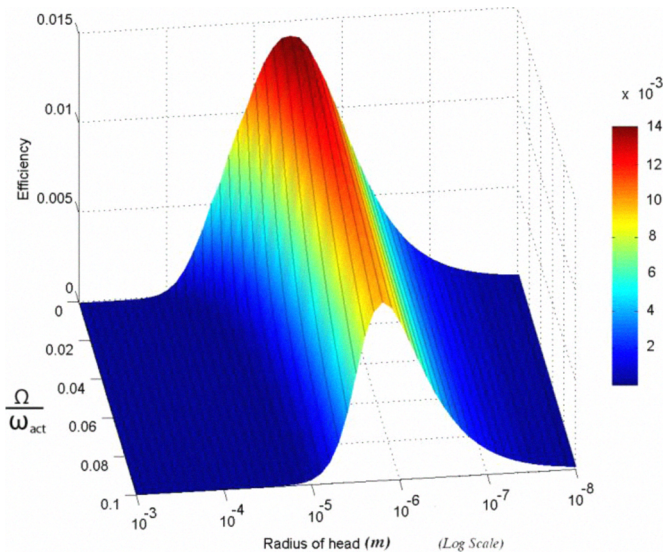


Fig. 3. Variation of efficiency with head size and  $(\Omega/\omega_{act})$  for the constant amplitude helical model in a medium with  $\mu = 4\text{mPa.s}$

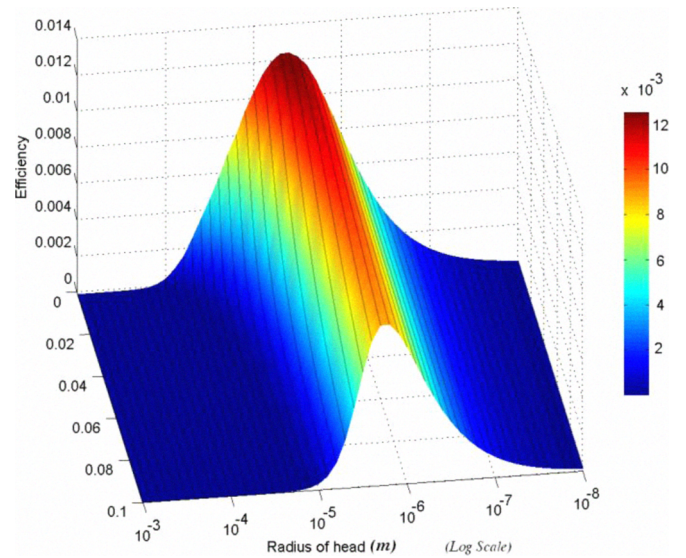


Fig. 4. Variation of efficiency with head size and  $(\Omega/\omega_{act})$  for the varying amplitude helical model in a medium with  $\mu=4\text{mPa.s}$

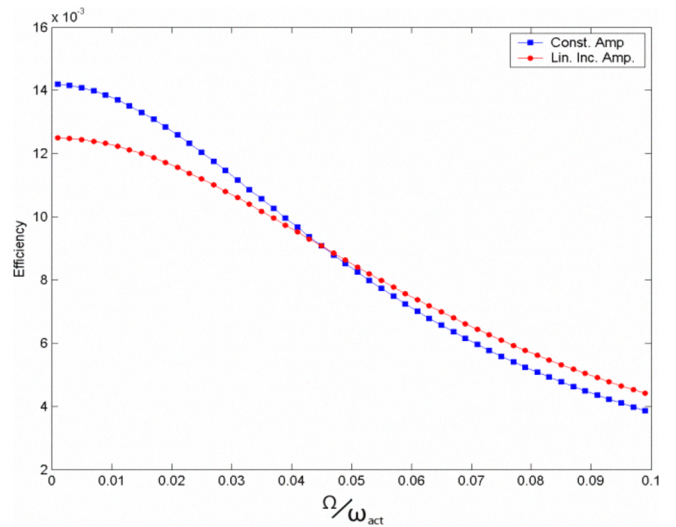


Fig. 5. Comparison between the efficiency of constant and varying amplitude helical models with the optimum head size, in a medium with  $\mu = 4\text{mPa.s}$

For the constant amplitude helical model, the variation of the efficiency with respect to size of the head and the ratio of the angular velocity of the head to that of the tail is obtained and plotted in Fig. 3. It is observed from the plot in Fig. 3, that the efficiency has a peak corresponding to an optimal head size for the condition of a stationary head ( $\Omega/\omega_{act} = 0$ ). Efficiency varies with changing  $\Omega/\omega_{act}$ . The optimal head size for maximum efficiency is a function of  $(\Omega/\omega_{act})$ . The varying amplitude model is presented for which the amplitude is

$$y = 2xM/np \quad (13)$$

where  $x$  is the distance from the head along the longitudinal axis,  $np$  is the total length along the longitudinal axis and  $M$  is the mean amplitude of the profile. The amplitude varies from zero and approaches its maximum value and the number of

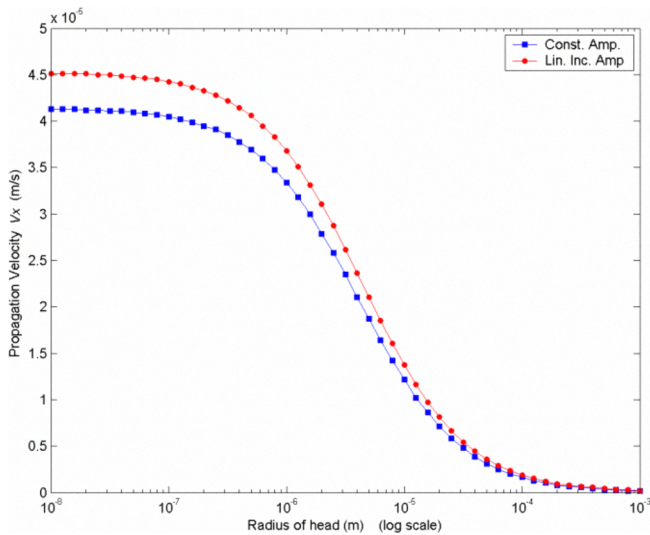


Fig. 6. Comparison of the propagation velocity in constant and varying amplitude helical models in a medium with  $\mu = 4\text{mPa}\cdot\text{s}$

turns, length of filament and the mean amplitude are kept the same as in the case of the constant amplitude helical flagellum.

The efficiency variation for linearly varying helical profile flagellar propulsion mechanism is shown in Fig. 4. The assumption of gradual increase in amplitude is valid for the linearly varying amplitude, with the angle between  $ds$  and  $dl$  being less than  $0.58^\circ$ . The nature of the plot is similar to that obtained for the constant amplitude case. Fig. 5 shows the variation of the efficiency with the angular velocity ratio for the optimum value of head size ( $\sim 3.98\ \mu\text{m}$ ) for the two considered cases of constant and linearly varying amplitude helix. The efficiency of the varying amplitude case is higher for  $\Omega/\omega_{\text{act}} > 0.047$  and the trend is opposite for the values lesser than 0.047. The propagation velocity is shown as a function of the head size for both the constant and variable amplitude helix in Fig. 6. The propagation velocity for the varying helix profile considered in the present work is higher than that for the constant amplitude helix. An increase in the viscosity leads to an increase in the thrust force but is balanced by an increase in the drag of the head. Therefore, variation in viscosity does not result in any change of parameters like velocity and efficiency. The model is valid only for the assumptions of viscous flow.

#### IV. CONCLUSION

An analytical model for propulsion attributed to generalized helical flagella has been developed. Keeping the mean amplitude constant, the linearly increasing amplitude helical model showed improved performance compared to the uniform amplitude model. Thus, a plausible design parameter for increased propagation of nanorobots is the helix profile. Apart from increment in velocity of nanorobot, the linear variation in amplitude reduces internal strains which may develop at the basal end of the flagella for constant amplitude helix.

Performance characteristics are a function of only dimensions and geometry of the helical flagella, where as, the thrust force experienced by the nanoswimmer changes with

viscosity and can potentially be used as a trigger in applications such as sensing and drug delivery [9].

The work may be extended to search and optimization of design parameters for increased efficiency in nanorobot propulsion. The model can be further improved by considering inter-flagellar interactions and its implications.

#### REFERENCES

- [1] N. N. Sharma and R. K. Mittal, "Nanorobot movement: Challenges and biologically inspired solutions," in *Proc. 4<sup>th</sup> Int. Conf. on Computational Intelligence, Robotics and Autonomous Systems*, Palmerston North, New Zealand, 2007, pp. 19-25.
- [2] E.M. Purcell, "Life at Low Reynolds Number," *American Journal of Physics*, vol. 45, pp. 3-11, 1977.
- [3] Johnson R. E. and Brokaw C. J., "Flagellar Hydrodynamics: A comparison between resistive force theory and slender body theory," *Biophysical Journal*, vol. 25, pp. 113-127, 1979.
- [4] Gray, J., and G. J. Hancock, "The propulsion of sea-urchin spermatozoa," *Journal of Experimental Biology*, vol. 32, pp. 802-814, 1955.
- [5] Brokaw C. J., "Flagellar Propulsion," *J. Exp. Biol.*, vol. 209(6), 2006, pp. 985-986.
- [6] Honda, T., Arai, K., and Ishiyama, K., 1999, "Effect of Micro Machine Shape on Swimming Properties of the Spiral-Type Magnetic Micro-Machine," *IEEE transaction on magnetics*, vol. 35, pp. 3688-3690.
- [7] B. Behkam and M. Sitti, "Modeling and testing of a biomimetic flagellar propulsion method for microscale biomedical swimming robots," in *Proc. Int. Conf. on Advanced Intelligent Mechatronics, IEEE/ASME*, Monterey, California, 2005, pp. 37-42.
- [8] B. Behkam and M. Sitti, "Design methodology for biomimetic propulsion of miniature swimming robots," *Journal of Dynamics Systems, Measurements, and Control*, Transactions of the ASME, vol. 128, pp. 36-43, 2006.
- [9] R. Majumdar, J. S. Rathore and N. N. Sharma, "Simulation of swimming nanorobots in biological fluids," in *Proc 4<sup>th</sup> Int. Conf. on Autonomous Robots and Agents*, New Zealand, 2009 (accepted).